NASA TECHNICAL NOTE

NASA TN D-5246

NASA TN D-5246

LINEARIZED THEORY OF STAGNATION POINT HEAT AND MASS TRANSFER AT HYPERSONIC SPEEDS

by Kenneth K. Yoshikawa

Ames Research Center
Moffett Field, Calif.

NATIONAL AERONAUTICS AND SPACE ADMINISTRATION • WASHINGTON, D. C. • AUGUST 1969

1. Report No. NASA TN D-5246	2. Government Accession No.	3. Recipient's Catalog No.
4. Title and Subtitle LINEARIZED THEORY OF STAGNATION POINT HEAT AND MASS TRANSFER AT HYPERSONIC SPEEDS		5. Report Date August 1969 6. Performing Organization Code
7. Author(s) Kenneth K. Yoshikawa		8. Performing Organization Report No. A-3260
9. Performing Organization Name and Address NASA Ames Research Center Moffett Field, Calif. 94035		10. Work Unit No. 129-01-02-05-00-21 11. Contract or Grant No. 13. Type of Report and Period Covered Technical Note
12. Sponsoring Agency Name and Address National Aeronautics and Space Administration Washington, D.C. 20546		14. Sponsoring Agency Code

15. Supplementary Notes

16. Abstract

An explicit closed-form solution has been obtained for the compressible, viscous shock-layer energy equation with mass addition or suction. The solution is applicable at very high speeds, when the interactions between the heated gas behind the shock wave and the layer of injected or ablated gases from the surface must be considered as well as the effect of heat conduction across the shock layer. The solution consists of the energy equation decoupled from the other conservation equations and then linearized by the introduction of constant values for the thermal and transport properties.

Results of using the solution show explicitly that the effect of gas injection on convective heat transfer depends on the Stanton number without mass addition and on the relative molecular weights, and thermal and transport properties of the free-stream and injected gases. The solution is substantiated by comparisons with more exact solutions.

17. Key Words (Suggested by Author)	18. Distribution Statement
Compressible flow Laminar flow Aerodynamic heat transfer Heat transfer Heat reduction by foreign gas injection	Unclassified - Unlimited

19. Security Classif. (of this report)	20. Security Classif. (of this page)	21. No. of Pages	22. Price
Unclassified	Unclassified	36	$3.00

LINEARIZED THEORY OF STAGNATION POINT HEAT AND MASS TRANSFER AT HYPERSONIC SPEEDS

By Kenneth K. Yoshikawa

Ames Research Center

SUMMARY

An explicit closed-form solution has been obtained for the compressible, viscous shock-layer energy equation with mass addition or suction. The solution is applicable at very high speeds, when the interactions between the heated gas behind the shock wave and the layer of injected or ablated gases from the surface must be considered as well as the effect of heat conduction across the shock layer. The solution consists of the energy equation decoupled from the other conservation equations and then linearized by the introduction of constant values for the thermal and transport properties.

Results of using the solution show explicitly that the effect of gas injection on convective heat transfer depends on the Stanton number without mass addition and on the relative molecular weights, and thermal and transport properties of the free-stream and injected gases. The solution is substantiated by comparisons with more exact solutions.

INTRODUCTION

A number of investigators (e.g., ref. 1) have suggested that reducing the bluntness of a vehicle will significantly decrease the severe radiative heating it encounters as it enters the earth's atmosphere at very high speeds. However, reducing the effective bluntness increases the convective heating to such a body. Thus, there is renewed interest in the problem of convective heat transfer, including the effects of mass addition employed for cooling.

Theoretical investigations of the effects of mass addition on convective heat transfer have been presented in references 2 through 20. The injection of nonreacting gases is generally treated by one of two fundamentally different approaches: (1) boundary-layer theory (refs. 2-5) and (2) shock-layer theory (refs. 6-8).

At altitudes and velocities associated with high-speed entry, it is necessary to employ shock-layer theory to analyze properly the problem of convective heating with mass addition. For high Reynolds number flow, Howe and Sheaffer (ref. 6) pointed out that, contrary to the results obtained from boundary-layer theory, the heat reduction due to mass addition was not simply correlated as a function of mass addition rate. For low Reynolds number

flow, Chen et al. (ref. 8) pointed out that the heat reduction due to mass addition was considerably different from that obtained with boundary-layer theory. Although the investigations based on shock-layer theory are useful, each problem, because of its complexity, requires a separate numerical solution.

With regard to the heat transfer, much of the complexity associated with the solutions to the shock-layer equations can be avoided if the energy equation is decoupled from the continuity and momentum equations. This approach seems plausible in light of recent results (refs. 21-23). Hanley and Korkan (refs. 21 and 22) showed that for inviscid flow, the normalized mass-flow distribution along the stagnation streamline was insensitive to radiative heat transfer in the shock layer. Matting (ref. 23) showed that for viscous flow along a cold wall, the mass-flow gradient in the boundary layer was essentially constant at the corresponding stagnation-point value.

The purpose of this report is to present a method for solving the shock-layer energy equation, decoupled from the continuity and momentum equations, by means of the results from references 21 to 23. (A similar method involving only radiative heating was presented in ref. 24.) Closed-form solutions of the energy equation are presented to demonstrate the dependence of convective heating on the appropriate physical parameters. In order to substantiate the present method, these solutions are compared, wherever possible, with numerical solutions obtained from the coupled equations. The primary effect of heat conduction in the shock layer on convective heating at the stagnation point is also incorporated in the analysis.

SYMBOLS

a parameter defined by equation (11c)

B blowing parameter, $\frac{\chi_w}{(St)_o}$

B_* characteristic blowing parameter (eqs. (B18) and (B19))

c mass fraction

c_p specific heat with constant pressure

D diffusion coefficient

erf error function

H free-stream total enthalpy, $h_\infty + \frac{1}{2} V_\infty^2$

h enthalpy

$\bar{h}$ dimensionless enthalpy, $\frac{h}{(H - h_w)}$

j total enthalpy, $h + \frac{1}{2}(u^2 + v^2)$

k	total thermal conductivity
k_a	constant defined in equation (B4)
k_b	constant defined in equation (B10)
k_w	effective ratio of mass-flow gradient (eq. (B9)), $\frac{(\chi_w')^{**}}{(\chi_w')^{*}}$
L	shock standoff distance
M	molecular weight of cold gas (at wall temperature)
Nu	Nusselt's number (eqs. (B25) and (B26))
$\overline{N}_f$	factor of proportionality defined in equations (19b) and (25b)
Pr	Prandtl number
p	pressure
q	heat flux
R	body radius
Re	Reynolds number
r	radial distance defined in figure 1
St	Stanton number, $\frac{q}{\rho_\infty V_\infty (H - h_w)}$
$(St)_r$	Stanton number for radiative heat flux, $\frac{q_r}{\rho_\infty V_\infty (H - h_w)}$
T	temperature
$\overline{T}$	$\frac{T}{T_s}$
u	x component of velocity
u_s	value of u at the shock, $V_\infty \frac{x}{R}$
V	velocity
v	y component of velocity
x	distance along body
y	distance normal to wall
β	Peclet number, $\frac{\rho_\infty V_\infty L}{(k/c_p)}$, (eq. (6b))
γ	modified factor of velocity gradient (eqs. (B4))

δ	boundary-layer thickness
$\delta^\dagger$	characteristic thickness
ϵ	density ratio across the shock wave, $\frac{\rho_\infty}{\rho_s}$
ζ	effective heat of ablation
η	normalized distance from wall, $\frac{y}{L}$
λ	parameter defined in equation (19b)
μ	viscosity
ρ	density
$\overline{\rho_\infty R}$	scaling factor for heat transfer normalized by value for $p_s = 1$ atm, $T_s = 15{,}000^\circ$ K, R = 1 ft
χ	dimensionless mass-flow parameter, $\frac{\rho v}{\rho_\infty V_\infty}$
χ'_w	absolute value of $\frac{\partial \chi}{\partial \eta}$ near the wall
ψ	convective heat reduction with gas injection, $\frac{q_c}{q_{co}}$

Superscripts

*	integrated quantity for the condition $T_s \gg T_w$ (e.g., eq. (9a))
**	quantity for the condition $T_s \simeq T_w$ (eq. (B5))

Subscripts

A,B	species A,B
c	convective
cr	critical
f	foreign gases or equivalent foreign gas
m	mixture
o	no blowing
r	radiative or reference conditions
ref	reference properties at $T = 15{,}000^\circ$ K

s condition just behind shock wave

w wall

δ boundary-layer edge

∞ free-stream gas or conditions

ANALYSIS

Conductive heat transfer will be considered with a simplified energy equation for the viscous, compressible flow in the neighborhood of a stagnation point. The thermodynamic and transport properties of the shock-layer gas will be introduced as averaged quantities. Solutions for the resulting linearized equation will be obtained for a body from which transpiration or ablation gases are emanating in hypervelocity flight. The calculation of the convective heat-transfer rate at the wall will be emphasized.

Assumptions and Geometry

The following assumptions are basic to the analysis (fig. 1 shows the geometry used in the analysis).

1. Steady axisymmetric stagnation-point flow
2. Thermodynamic equilibrium
3. No chemical reactions between free-stream and injection or ablation gases
4. Thermal radiation uncoupled (convective heat can be derived separately by means of the driving enthalpy)
5. Laminar continuum flow
6. Thin shock layer, $L/R \ll 1$
7. Small blowing rates, $\rho_w v_w \ll \rho_\infty V_\infty$
8. Thermal diffusion and diffusion-thermal neglected

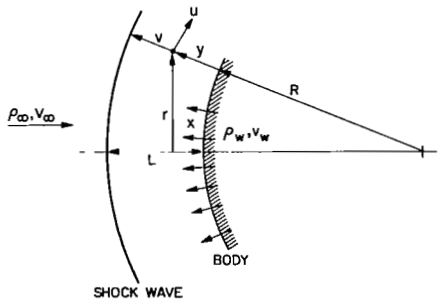

Figure 1.- Flow geometry.

Basic Equations

Conservation equations for steady flow of multicomponent chemically reacting gases in the shock layer have been derived previously (see, e.g., refs. 5, 25-27). The resulting equations (discussed in detail in ref. 26) for the conditions of the present analysis are:

Continuity equation

$$\frac{\partial}{\partial x}(\rho u r) + \frac{\partial}{\partial y}(\rho v r) = 0 \tag{1a}$$

Momentum equation

$$\rho u \frac{\partial u}{\partial x} + \rho v \frac{\partial u}{\partial y} = -\left(\frac{\partial p}{\partial x}\right) + \frac{\partial}{\partial y}\left(\mu \frac{\partial u}{\partial y}\right) \tag{1b}$$

$$\frac{\partial p}{\partial y} = 0 \tag{1c}$$

Energy equation

$$\rho u \frac{\partial j}{\partial x} + \rho v \frac{\partial j}{\partial y} = \frac{\partial}{\partial y}\left(k \frac{\partial T}{\partial y}\right) + \frac{\partial}{\partial y}(q_r) \tag{2}$$

Diffusion equation for the binary system

$$\rho u \frac{\partial c_f}{\partial x} + \rho v \frac{\partial c_f}{\partial y} = \frac{\partial}{\partial y}\left(\rho D_f \frac{\partial c_f}{\partial y}\right) \tag{3}$$

Since the major portion of this study is concerned with convective heat transfer to the stagnation point, the energy equation for the shock-layer flow is further simplified, for $\rho u(\partial j/\partial x) \ll \rho v\,(\partial j/\partial y)$ and $(1/2)(u^2 + v^2) \ll h$,

$$\rho v \frac{\partial h}{\partial y} = \frac{\partial}{\partial y}\left(\frac{k}{c_p} \frac{\partial h}{\partial y}\right) + \frac{\partial}{\partial y}(q_r) \tag{4}$$

Equation (4) can be decoupled from the continuity and momentum equations (1) by the introduction of a normalized mass-flow distribution which is independent of the heat transfer.

Normalized Mass-Flow Distribution

The mass-flow distribution along the stagnation streamline must be determined to decouple the energy equation. For inviscid, nonadiabatic flow, Hanley (refs. 21 and 22) showed that the normalized mass-flow distribution, $\chi = \rho v/\rho_\infty V_\infty$, is relatively insensitive to radiation transport. For boundary-layer flow, Matting (ref. 23) demonstrated that the mass-flow

gradient through the highly compressed boundary layer was essentially constant. These two results suggest that the mass-flow profile throughout the shock layer (viscous and nonadiabatic) is also relatively independent of the heat transfer, an assumption substantiated by a number of published papers (refs. 6, 7, 26, 28, and 29). (Note that the flow-field solutions in refs. 6, 7, and 26 include mass addition in the stagnation region.) Thus, the effective mass-flow equation will be written as

$$\chi \equiv \frac{\rho v}{\rho_\infty V_\infty} = \chi_w - \chi_w' \eta - (1 - \chi_w' + \chi_w)\eta^2 \tag{5}$$

where $\eta = y/L$ is the distance from the wall normalized by the shock stand-off distance. It should be noted that χ_w' is the absolute value of $(\partial\chi/\partial\eta)$ a short distance away from the wall since the wall value is zero. One is justified in this approach because χ_w' does not directly affect the heat transfer (see eq. (8)) and $\partial\chi/\partial\eta$ is essentially constant through the boundary layer except very near the wall (see, e.g., refs. 23 and 26, figs. 8 and 2, respectively). It will be assumed that χ_w' is independent of the blowing rate but a function of the body shape and density ratio across the normal shock.

General Solution of Energy Equation

From equations (4) and (5) the dimensionless energy equation for the shock layer becomes

$$\chi \frac{d\bar{h}}{d\eta} = \frac{d}{d\eta}\left(\frac{1}{\beta}\frac{d\bar{h}}{d\eta}\right) + \frac{d(St)_r}{d\eta} \tag{6a}$$

where dimensionless quantities are defined as

$$\left.\begin{aligned} \bar{h} &= \frac{h}{H - h_w} \\ (St)_r &= \frac{q_r}{\rho_\infty V_\infty (H - h_w)} \\ \beta &= \frac{\rho_\infty V_\infty L}{k/c_p} \end{aligned}\right\} \tag{6b}$$

and H is the adiabatic enthalpy behind the shock wave. For simplicity, equation (6a) may be solved by treating separately the effects of conduction and radiation on the flow enthalpy. The case where radiation is predominant has been studied in reference 24. The analysis in this report is concerned with the case where conduction is predominant.

The energy equation and boundary conditions, neglecting radiation become

$$\chi \frac{d\bar{h}}{d\eta} = \frac{d}{d\eta}\left(\frac{1}{\beta}\frac{d\bar{h}}{d\eta}\right) \tag{7a}$$

$$\left.\begin{aligned} \bar{h} &= \bar{h}_w \quad \text{at} \quad \eta = 0 \\ \bar{h} &= \bar{h}_s \quad \text{at} \quad \eta = 1 \end{aligned}\right\} \tag{7b}$$

A general solution to equation (7a) and boundary conditions (7b) may be written

$$\bar{h} - \bar{h}_w = (St) \int_0^{\eta} \beta e^{\int_0^{\eta_1} \beta\chi \, d\eta_2} \, d\eta_1 \tag{8a}$$

where

$$(St) \equiv \frac{1}{\beta_w}\left(\frac{d\bar{h}}{d\eta}\right)_w = \frac{\bar{h}_s - \bar{h}_w}{\displaystyle\int_0^{1} \beta e^{\int_0^{\eta_1} \beta\chi \, d\eta_2} \, d\eta_1} \tag{8b}$$

Equations (8) are nonlinear solutions since β depends upon the unknown function $\bar{h}$. Generally, the analytical evaluation of this equation is extremely difficult.

Linearized Solution of Energy Equation

A linearized solution to the energy equation can be given explicitly when the Peclet number β is replaced by an average value. For the condition of constant pressure and $T_w \ll T_s$, let

$$\left(\frac{k}{c_p}\right)^* = \frac{1}{T_s}\int_0^{T_s} \frac{k}{c_p} \, dT \tag{9a}$$

and

$$\beta^*(T_s) = \frac{\rho_\infty V_\infty L}{(k/c_p)^*} \tag{9b}$$

The linearized solution thus becomes

$$\bar{h} - \bar{h}_w = \left(\frac{d\bar{h}}{d\eta}\right)_w \int_0^{\eta} e^{\beta^* \int_0^{\eta_1} \chi \, d\eta_2} \, d\eta_1 \tag{10a}$$

where

$$\left(\frac{d\bar{h}}{d\eta}\right)_w = \frac{\bar{h}_s - \bar{h}_w}{\int_0^1 e^{\beta^* \int_0^{\eta_1} \chi \, d\eta_2} \, d\eta_1} \tag{10b}$$

A vigorous mathematical justification of the substitution of this average function in the nonlinear energy equation is beyond the scope of this report. However, the method is substantiated later where the numerical results of convective heat transfer from the solutions of other investigators (refs. 6, 26, 30) and also from the exact solution of equations (8) show excellent agreement with the present linearized solutions. Incorporating equation (5) in equations (10), one obtains

$$\frac{d\bar{h}}{d\eta} = \left(\frac{d\bar{h}}{d\eta}\right)_w e^{-\beta^*\left[-\chi_w \eta + (1/2)\chi_w' \eta^2 + (1/3)(1 - \chi_w' + \chi_w)\eta^3\right]} \tag{11a}$$

when $\beta^* >> 1$, the entire exponential tends to zero. Furthermore, when η is small, the last term in the exponent can be neglected. This allows the integral of equation (11a) to be expressed in terms of the error function

$$\bar{h} = \frac{(\bar{h}_s - \bar{h}_w)\operatorname{erf}\left[\sqrt{\frac{1}{2}(\beta\chi_w')^*}\,\eta - a\right] + \bar{h}_s \operatorname{erf} a + \bar{h}_w \operatorname{erf}\left[\sqrt{\frac{1}{2}(\beta\chi_w')^*} - a\right]}{\operatorname{erf}\left[\sqrt{\frac{1}{2}(\beta\chi_w')^*} - a\right] + \operatorname{erf} a} \tag{11b}$$

where

$$a = \sqrt{\frac{1}{2}\left(\frac{\beta}{\chi_w'}\right)^*}\,\chi_w \tag{11c}$$

Furthermore, for χ_w small and $\beta^* >> 1$,

$$\operatorname{erf}\left[\sqrt{\frac{1}{2}(\beta\chi_w')^*} - a\right] \simeq 1$$

It follows then from equations (11) that

$$\left(\frac{d\bar{h}}{d\eta}\right)_w = \sqrt{\frac{2}{\pi}\,(\beta\chi_w')^*}\;(\bar{h}_s - \bar{h}_w)\;\frac{e^{-a^2}}{1 + \operatorname{erf} a} \tag{12a}$$

The convective heat is, by definition,

$$q_c = \left(\frac{k}{c_p}\frac{\partial h}{\partial y}\right)_w = \frac{\rho_\infty V_\infty (H - h_w)}{\beta^*}\left(\frac{d\bar{h}}{d\eta}\right)_w \tag{12b}$$

Thus,

$$q_c = \sqrt{\frac{2}{\pi}\left(\frac{\chi_w'}{\beta}\right)^*}\;\rho_\infty V_\infty (h_s - h_w)\;\frac{e^{-(1/2)(\beta/\chi_w')^*\chi_w^2}}{1 + \operatorname{erf}\left[\sqrt{\frac{1}{2}\left(\frac{\beta}{\chi_w'}\right)^*}\;\chi_w\right]} \tag{13}$$

For the no injection case $\chi_w \to 0$, and equation (13) can be written

$$q_{co} = \sqrt{\frac{2}{\pi}\left(\frac{\chi_w'}{\beta_o}\right)^*}\;\rho_\infty V_\infty (h_s - h_w) \tag{14}$$

where

$$\beta_o^* \equiv \frac{\rho_\infty V_\infty L_o}{(k/c_p)^*}$$

A blowing parameter and a Stanton number for the no injection case can be defined as

$$B = \frac{\chi_w}{(St)_o} \tag{15a}$$

$$(St)_o \equiv \frac{q_{co}}{\rho_\infty V_\infty (H - h_w)} \simeq \sqrt{\frac{2}{\pi}\left(\frac{\chi_w'}{\beta_o}\right)^*} \qquad \text{for} \quad \frac{h_w}{h_s} \ll 1 \tag{15b}$$

Equations for Heat Reduction

The heat reduction due to foreign gas injection is obtained in terms of the blowing parameter B by dividing equation (13) by equation (14) and using the definition (15a).

$$\psi = \frac{q_c}{q_{co}} = \frac{1}{\sqrt{\frac{L}{L_o}\frac{(\chi_w' k/c_p)^*_\infty}{(\chi_w' k/c_p)^*_m}}} \left[\frac{e^{-\frac{1}{\pi}\frac{L}{L_o}\frac{(\chi_w' k/c_p)^*_\infty}{(\chi_w' k/c_p)^*_m} B^2}}{1 + \operatorname{erf}\sqrt{\frac{1}{\pi}\frac{L}{L_o}\frac{(\chi_w' k/c_p)^*_\infty}{(\chi_w' k/c_p)^*_m}}\, B} \right] \tag{16}$$

where subscripts ∞ and m refer to properties of the free-stream gas in the shock layer for no injection and properties of the mixture of gases in the shock layer for injection, respectively. The closed form solution (eq. (16)) can be used to deduce the ratio of the parameter $(\chi_w' k/c_p)^*_\infty/(\chi_w' k/c_p)^*_m$ from either experimental data or the results of numerical calculations (e.g., refs. 3 and 4).

Identical-gas injection.- With the assumption that $(\chi_w')^*$ is independent of blowing, it follows directly for identical-gas injection that

$$\frac{(\chi_w' k/c_p)^*_\infty}{(\chi_w' k/c_p)^*_m} \simeq 1$$

Then ψ is written

$$\psi = \sqrt{\frac{L_o}{L}} \left[\frac{e^{-\frac{1}{\pi}\frac{L}{L_o} B^2}}{1 + \operatorname{erf}\sqrt{\frac{1}{\pi}\frac{L}{L_o}}\, B} \right] \tag{17}$$

Equation (17) provides remarkable agreement with more exact solutions as shown in the Results and Discussion section.

For the case $L/L_o \simeq 1$, such as for a large body with a thin boundary layer, equation (17) may be expanded in a series as

$$\psi \simeq 1 - \frac{2}{\pi} B + \ldots \tag{18}$$

Equation (18) compares very well with the empirical formula suggested by others (refs. 2, 3, 9, 10).

Single foreign gas injection.- The property, $(k/c_p)^*_m$ in equation (16) refers to the mixture of gases in the shock layer and as such it depends on both the individual thermal and transport properties and the local mass concentrations of the species. Therefore, an exact evaluation of this property would entail a solution to the species equation and moreover necessitate the computation of high temperature transport properties which requires physical

constants still not well established (refs. 11, 14, 18, 31-37). Since the primary interest here is to obtain a simple heat-transfer formula for engineering use, the above difficulties will be avoided by introducing the following approximation

$$\frac{(\chi'_w k/c_p)^*_\infty}{(\chi'_w k/c_p)^*_m} \simeq \begin{cases} \left[\dfrac{(\chi'_w k/c_p)^*_\infty}{(\chi'_w k/c_p)^*_f}\right]^{B/B_*} & \text{for } 0 \le B \le B_* \\ \dfrac{(\chi'_w k/c_p)^*_\infty}{(\chi'_w k/c_p)^*_f} & \text{for } B > B_* \end{cases} \tag{19a}$$

where B_* is the blowing parameter for the boundary-layer blow-off defined in appendix B. Equation (19a) has the proper physical behavior since it weights the properties of the foreign gas according to the magnitude of B for $B \lesssim B_*$ and is constant for $B \gtrsim B_*$ where the foreign gas is dominant over the main stream gas.

Since $(k/c_p)^* \propto \sqrt{M}$, the parameter λ may be defined by

$$\lambda \equiv \frac{(\chi'_w k/c_p)^*_\infty}{(\chi'_w k/c_p)^*_f} = \sqrt{\frac{M_\infty}{M_f}}\,\bar{N}_f \tag{19b}$$

where $\bar{N}_f$ is a weighting factor which depends on the type of foreign gas. By the present method in conjunction with the numerical results of reference 3, the factor $\bar{N}_f$ was found to be (for air as the main stream)

$$\begin{cases} \bar{N}_f \simeq \dfrac{5}{9} & \text{for monatomic gas} \\ \bar{N}_f \simeq 1 & \text{for diatomic and polyatomic gases} \end{cases} \tag{19c}$$

Derivations of these values will be discussed in detail in the Results and Discussion section.

Equation (16), in conjunction with equations (19a) and (19b), therefore, leads to

$$\psi \simeq \left[\frac{L}{L_o}\lambda^{(B/B_*)}\right]^{-1/2} \frac{e^{-\frac{1}{\pi}\frac{L}{L_o}\lambda^{(B/B_*)}B^2}}{1 + \operatorname{erf}\left[\frac{1}{\pi}\frac{L}{L_o}\lambda^{(B/B_*)}\right]^{1/2} B} \qquad \text{for } B \le B_* \tag{20a}$$

$$\psi \simeq \left(\frac{L}{L_o}\lambda\right)^{-1/2} \frac{e^{-\frac{1}{\pi}\frac{L}{L_o}\lambda B^2}}{1 + \operatorname{erf}\left(\frac{1}{\pi}\frac{L}{L_o}\lambda\right)^{1/2} B} \qquad \text{for } B > B_* \tag{20b}$$

Equations (20) provides excellent agreement with the results of reference 4.

It is interesting that if the empirical form of the blowing parameter suggested by a number of authors for the case of foreign gas injection (i.e., replace B by $(M_\infty/M_f)^{1/4}$ B) is used, equation (17) immediately leads to

$$\psi = \left(\frac{L}{L_o}\right)^{-1/2} \frac{e^{-\frac{1}{\pi}\frac{L}{L_o}\left(\frac{M_\infty}{M_f}\right)^{1/2}B^2}}{1 + \operatorname{erf}\sqrt{\frac{1}{\pi}\frac{L}{L_o}\left(\frac{M_\infty}{M_f}\right)^{1/2}}\, B} \tag{21}$$

where M_f is the molecular weight of the foreign gas. Equation (21) provides very satisfactory results for most single foreign gas injectants (hydrogen excepted).

Mixed foreign gas injection.- When injected gases consist of two or more gases, the calculation of the transport properties is further complicated. A reciprocal formula for the equivalent transport properties is applied, that is,

$$\frac{1}{(\chi_w' k/c_p)_f^*} = \frac{c_A}{(\chi_w' k/c_p)_A^*} + \frac{c_B}{(\chi_w' k/c_p)_B^*} \tag{22a}$$

where A and B refer to the injected gases and are their respective mass fractions. Incorporating equation (22a) in equation (19b),

$$\lambda = \sqrt{\frac{M_\infty}{M_A}}\,\bar{N}_A\left(c_A + c_B\sqrt{\frac{M_A}{M_B}}\,\frac{\bar{N}_B}{\bar{N}_A}\right) \tag{22b}$$

This may be written in terms of the equivalent molecular weight M_f and $\bar{N}_f$ as

$$\lambda = \sqrt{\frac{M_\infty}{M_f}}\,\bar{N}_f \tag{22c}$$

where

$$\left.\begin{aligned} \frac{1}{M_f} &= \frac{c_A}{M_A} + \frac{c_B}{M_B} \\ \bar{N}_f &= c_A\left(\sqrt{\frac{M_f}{M_A}}\,\bar{N}_A\right) + c_B\left(\sqrt{\frac{M_f}{M_B}}\,\bar{N}_B\right) \end{aligned}\right\} \tag{22d}$$

Substituting equations (22) into equations (20), ψ for the case of the mixed gas injection is obtained. As can be recognized from equations (22), the equivalent molecular weight consisting of two or more different gases does not itself provide the same result for a single gas with the same molecular weight. It will be shown later that equations (20) and (22) provide close agreement with the numerical solutions of reference 4 when more than one gas is injected.

Ablation.- For forced injection the blowing rate parameter is given a priori and the solution is straightforward. For ablation, however, the blowing rate parameter depends on the heat transfer to the wall, and the solution is, therefore, coupled. The mass loss rate of ablation vapors per unit area is given by

$$-\frac{dm}{dt} = \rho_w v_w = \psi\,\frac{q_{co}}{\zeta} \tag{23a}$$

where ζ is the effective heat of ablation. With the definition of B given in equations (15), equation (23a) may be rewritten

$$\psi = \left(\frac{\zeta}{H - h_w}\right) B \tag{23b}$$

Ideally, equations (16) and (23b) may be combined to eliminate B (or ψ) and to obtain ψ (or B) for ablation. However, a more practical approach is to obtain graphical solutions by superimposing equation (23b), which represents a family of straight lines with the slope $\zeta/(H - h_w)$, on equations (20) for ψ calculated for the forced injection.

Effect of Heat Conduction Behind the Shock

The enthalpy immediately behind a strong shock wave will be significantly altered by heat transfer at the wall when conductive heat becomes a major

factor in the energy balance across the bow shock wave. The effect of conductive heat on the energy balance is to reduce the flow enthalpy behind the shock; this phenomenon is designated here as the "postcooling effect," in contrast to the preheating effect which increases the flow enthalpy behind the shock (ref. 24). Only preliminary effects of heat transfer on the viscous flow field and on the convective heat at the stagnation point will be discussed (see Results and Discussion). A brief analysis of the reduction in heat transfer due to the postcooling effect is described in appendix A.

Approximate Equations for the Flow Properties

The various physical quantities required to evaluate the linearized solutions are given, or derived, in detail in appendix B: These quantities are the mass-flow gradient, shock-layer thickness, boundary-layer thickness, boundary-layer blow-off parameter, and the heat-transfer parameter.

RESULTS AND DISCUSSION

Calculations of the average transport properties, the convective heat-transfer rate at the stagnation point with suction or foreign gas injection, the heat-transfer parameter in the vicinity of the stagnation point, and the mass-flow gradient for the higher wall temperature are presented in this section for atmospheric flight conditions at very high speeds. Also considered is the postcooling effect on the convective heating rate at low Reynolds numbers.

Thermal and Transport Properties

The thermal and transport properties for air reported by Hansen (ref. 31) are employed because the present analysis will be compared with numerical solutions using these properties, and changes in the properties at the higher temperatures as reported recently (refs. 34-37) should not significantly affect the conclusions of the present analysis.

Normalized values of k/c_p are shown in figure 2(a) as functions of temperature for various pressure levels. (For simplicity in plotting, the reference condition is based on $T_{ref} = 15{,}000^\circ$ K.) Also shown are the averaged values, $(k/c_p)^*$, calculated by equation (9a). The parameter $(k/c_p)^*$ can be approximated by a straight line which passes through the origin and a reference value at a lower temperature. (See tables I and II for numerical values.)

Figure 2(b) presents the average parameter $(k/c_p)^*$ plotted against enthalpy at 1000° K intervals. It can be seen that $(k/c_p)^*$ may be approximated by the square root of the enthalpy. This also follows from the previous figure since temperature is approximately proportional to the square root of the enthalpy (see, e.g., fig. 2 of ref. 24).

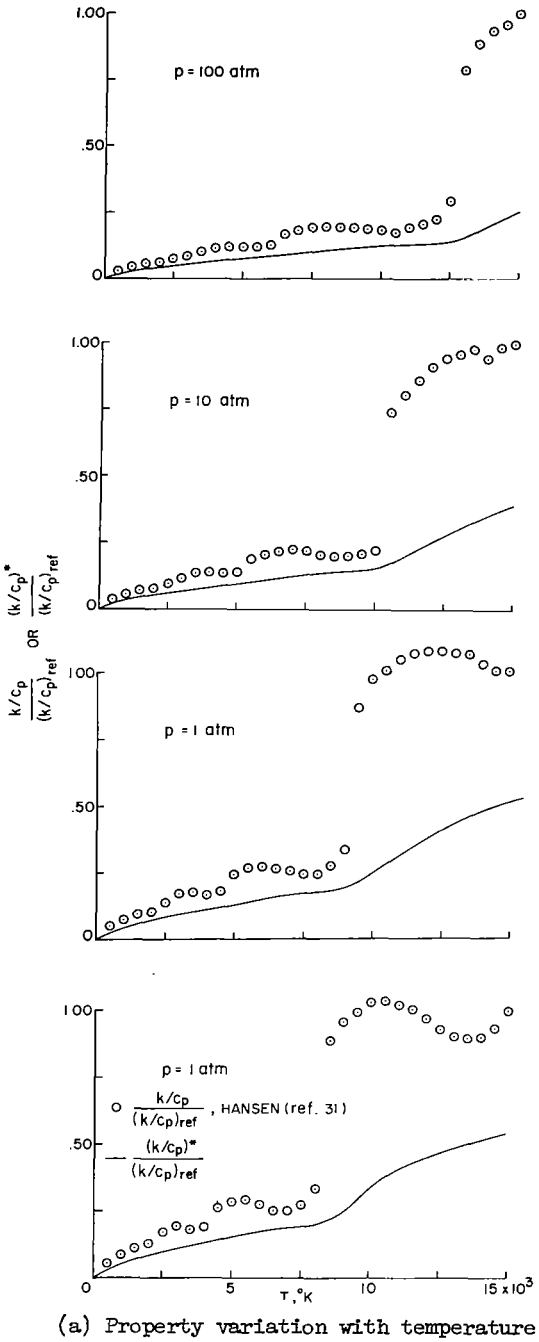

(a) Property variation with temperature.

Figure 2.- Thermal and transport property parameter for air.

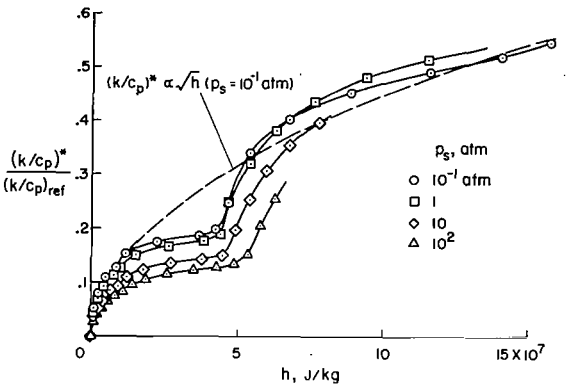

(b) Average-property variation with enthalpy.

Figure 2.- Concluded.

The results found from figure 2 bear an important consequence; namely, the thermal-transport property parameter can be approximated by

$$\left(\frac{k}{c_p}\right)^* \simeq \left(\frac{k}{c_p}\right)_r^* \sqrt{\frac{h}{h_r}} \propto \left(\frac{k}{c_p}\right)_r^* V_\infty \qquad (24a)$$

where h_r is the reference enthalpy at a lower temperature (a constant for all gases).[1] Incorporating equation (24a) with equation (14), one can derive the important equation (see eq. (B22)).

$$q_{co}\sqrt{\frac{R}{p_s}} \simeq \sqrt{\frac{\sqrt{2}}{\pi}\frac{(\chi_w^f k/c_p)_r^*}{k_a \epsilon (h_r)^{1/2}}}\,(h_s - h_w) \qquad (24b)$$

Equation (24b) shows that the convective heat transfer at high

[1]That is, $h_r \simeq 1700$ Btu/lb ($\simeq 4$ MJ/kg). However, the reference enthalpy at a higher temperature which provides the same result in equations (24) is $h_r \simeq 27{,}000$ Btu/lb ($\simeq 63$ MJ/kg) for all gases. As will be recognized later, the parameter used in equation (19b) can be deduced more precisely from the figures at the higher h_r than the lower h_r.

temperatures can be expressed in terms of gas properties at a lower temperature. Marvin and Pope arrived at the same result for air and other gases. Equations (24) further provide the following important relations: Equation (19b), with equations (24), becomes

$$\lambda \simeq \frac{[(\chi_w' k/c_p)^*_\infty]_r}{[(\chi_w' k/c_p)^*_f]_r} \simeq \frac{(q_{co}\sqrt{R/p_s})^2_\infty}{(q_{co}\sqrt{R/p_s})^2_f} \tag{25a}$$

Since $(k/c_p)^*_r \propto \sqrt{M}$ at the lower temperature, where M is the molecular weight of the cold gas, the factor of proportionality $\bar{N}_f$ is related by

$$\lambda = \sqrt{\frac{M_\infty}{M_f}}\,\bar{N}_f \simeq \frac{(q_{co}\sqrt{R/p_s})^2_\infty}{(q_{co}\sqrt{R/p_s})^2_f} \tag{25b}$$

The values of $\bar{N}_f$ given in equation (19c), and equation (22c) for gas mixtures, can therefore be determined from figure 5 in reference 3.

Results Without Postcooling

Laminar convective heat transfer without injection.- The results for no postcooling obtained from equations (B3), (B6), and (B21) are shown in figure 3(a) along with the predictions of Hoshizaki (ref. 30), Fay and Riddell (ref. 38), and Howe and Viegas (ref. 26). Typical results from other studies may be found in references 39 to 43. The present results show a slight but noticeable dependency on pressure level. They agree well with the numerical results of Howe and Viegas for $p_s = 1$ atm, and approach the result of Hoshizaki for lower pressure.

The heat-transfer parameter $Nu/\sqrt{Re}\,|_x$ calculated from equation (B27) assuming $(\chi_w')^* \simeq 1/2$ is shown in figure 3(b) for $p_s = 1$ atm. The present

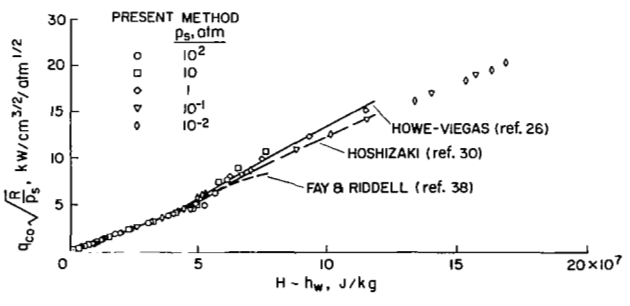

(a) Convective heating rate.

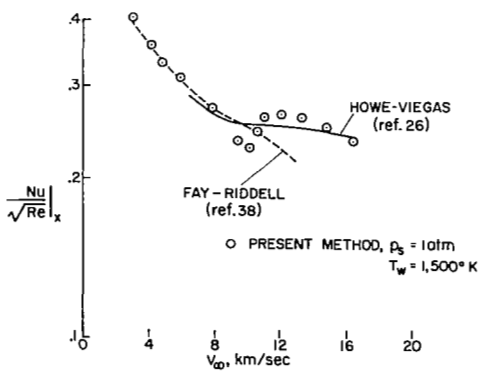

(b) Nusselt number.

Figure 3.- Stagnation-point heat transfer for air.

analysis provides remarkably good agreement with the results of Fay and Riddell for the lower flight speeds and with the results of Howe and Viegas for the higher flight speeds.

Mass-flow gradients.- The effect of wall temperature on the normalized mass-flow gradient is demonstrated in figure 4 for specified conditions. The quantity k_w, the effective ratio of the mass-flow gradient for the hot wall to that for the cold wall, deduced from reference 23, is compared with the present result (eq. (B8)) for the condition of the lower stagnation temperature. The effective mass-flow gradient decreases as the wall temperature increases because of the effect of higher viscosity in the boundary layer. Also presented is the result for the higher stagnation temperature (T_s = 15,000° K, p_s = 1 atm) which demonstrates a further decrease in the effective velocity gradient.

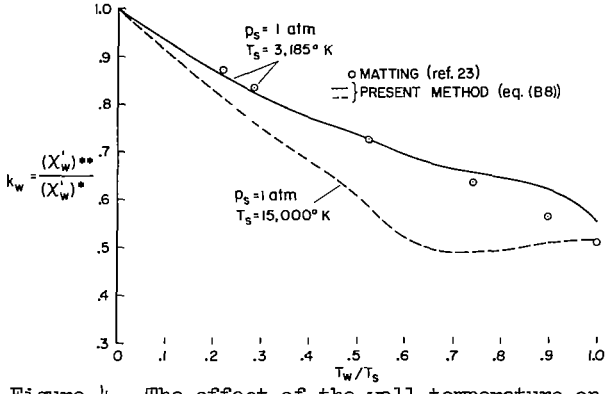

Figure 4.- The effect of the wall temperature on mass flow gradient (air).

Heat reduction - identical gas injections.- A comparison of the present solution (eq. (17)) for $\overline{\rho_\infty R} = 1$ with the more exact numerical solutions of Howe and Sheaffer (ref. 6), and with the correlation of numerical solutions by Marvin and Pope (ref. 3), whose results are identical to those of reference 2, is presented in figure 5 for identical gas injections. The present results show excellent agreement with all of the numerical solutions. Also presented is the linear equation (18) which agrees with the empirical equations of references 9 and 10 and is very close to the linearized solution for $B < 1$. Note that the ψ function is independent of the boundary temperatures T_s and T_w (eq. (17)). However, the present solution shows that the ψ function is not a single curve, but depends upon the stagnation-point Stanton number $(St)_o$ or the product of the ambient density and body radius $\overline{\rho_\infty R}$ as shown next.

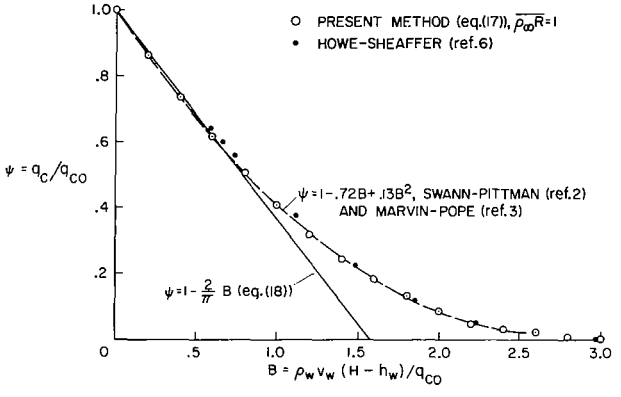

Figure 5.- Heat reduction with identical gas injection.

Scaling factor for correlation.- As the product of the density and the body radius decreases, the mass transfer becomes more effective in reducing the heat transfer, as illustrated in figure 6. The product $\overline{\rho_\infty R}$ in the figure has been normalized by the value for p_s = 1 atm, T_s = 15,000° K, and R ≃ 30 cm (1 ft). The present solutions and those of Howe and Sheaffer

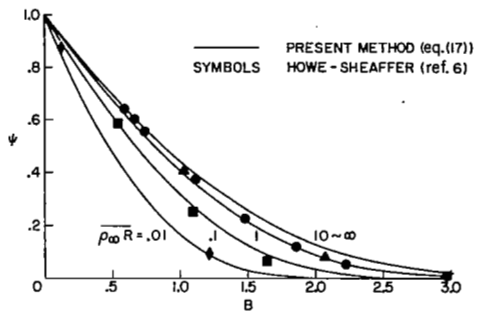

Figure 6.- Heat reduction for air with scaling factor.

(ref. 6)[2] agree well. A single correlation curve for the shock-layer theory can be obtained only if the product $\overline{\rho_\infty R}$ remains constant. This scaling effect on heat transfer is easily recognized from equations (17), (B11), and (B12). Boundary-layer theory, on the other hand, provides one correlation curve of the blowing effectiveness, independent of the product $\overline{\rho_\infty R}$ (e.g., refs. 2-4). For large values of $\overline{\rho_\infty R}$, the shock-layer and boundary-layer theories seem to provide similar results. The present results and those of Howe and Sheaffer and of Marvin and Pope (also refs. 2 and 4) agree well, as illustrated in the previous figure. This is a condition for which the shock-layer thickness changes only a small amount as a result of gas injection. Changes in the shock-layer thickness resulting from transpiration or gas injection are significant for low values of $\overline{\rho_\infty R}$ (but still in the continuum regime without the postcooling effect) and are accompanied by changes in the velocity gradient at the stagnation point. The present shock-layer solutions account for the changes in the shock layer thickness, as do those of Howe and Sheaffer and of Goldberg and Scala.

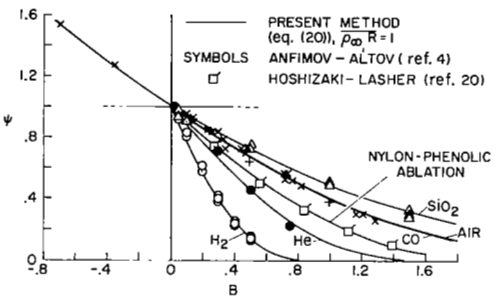

Figure 7.- Heat reduction in air with single foreign gas injection.

Heat reduction - foreign gas injection.- Injection of gases different from the free-stream gas affects the heat transfer in the manner shown in figure 7. The present results for $\overline{\rho_\infty R}$ = 1.0 using equations (20) are compared with the boundary-layer solutions from references 4 and 20. Very good agreement is obtained with the solutions of Anfimov and Al'tov for "single foreign gases" (non-mixed) over the entire blowing rate range (including suction) and equally good agreement is obtained with the solutions of Hoshizaki and Lasher (ref. 20) for nylon phenolic ablation. The injection of light gases is more effective in reducing the heat transfer provided no combustion takes place.

The dependence of the effectiveness of transpiration upon the Stanton number (or free-stream density and body radius) is also a function of the molecular weight of the injectant gas relative to that of the free-stream gas.

---

[2]Those numerical solutions that were misplotted in figure 5 of reference 6 have been corrected in figure 6 of this report.

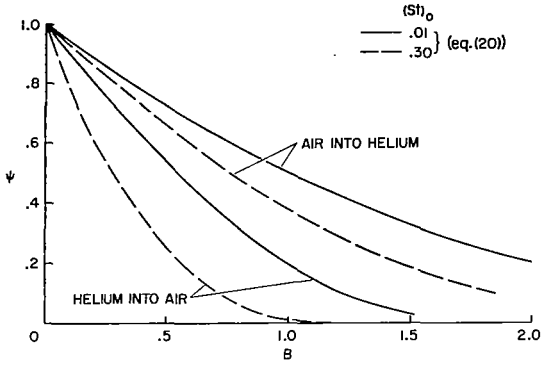

Figure 8.- Heat reduction for different free-stream gases.

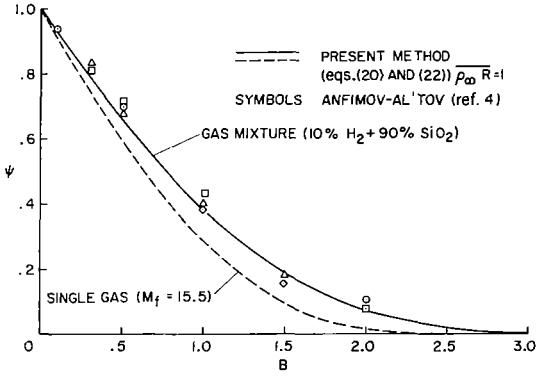

Figure 9.- Heat reduction with mixed foreign gas injection.

For example, figure 8 indicates that changes in the Stanton number affect the heat transfer more for the injection of helium into air than for the injection of air into helium. Again, this is to be expected on the basis of changes in the shock-layer thickness; a given amount of helium injected into an air stream increases the shock-layer thickness more than the same amount of air injected into a helium stream (see eq. (B10)).

Figure 9 shows how injecting a "gas-mixture" affects heat transfer. For transpiration of a mixture of a light gas and a heavy gas, the gas near the wall, which is the heavy gas, predominates so that the mixture is less effective in reducing the heat transfer than a single gas[3] of the same molecular weight. The dashed curve represents the result obtained for a single polyatomic gas of the same molecular weight. The results of the present method, using the reciprocal of the equivalent transport relation (see eqs. (22)), agree well with the numerical results of Anfimov and Al'tov. Anfimov and Al'tov proposed the simple formula:

$$\psi \simeq \pi_i \psi_i \tag{26}$$

that is, the net heat reduction by the mixture is the cross product of the individual heat reductions for each species (ref. 4). However, this equation is good only for small values of the blowing parameter.

Effect of Postcooling on Convective Heat Transfer

The effect of postcooling on the stagnation-point flow is to reduce the driving enthalpy, and thereby lower the convective heat at the body surface. (The vorticity at a low Reynolds number increases the convective heating (e.g., refs. 6 and 44), and thus tends to counteract the postcooling effect.) An exploratory study of this effect is presented here.

---

[3]Single monatomic (polyatomic) gas if the mixture is made up with more than two monatomic (polyatomic) gases.

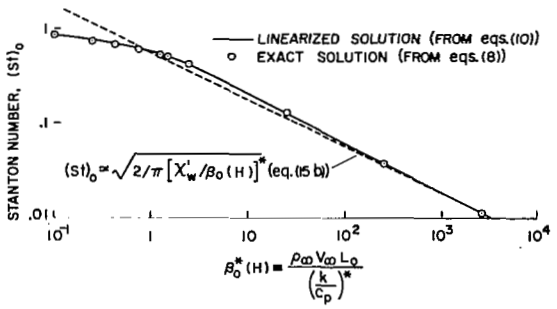

(a) Stanton number without injection.

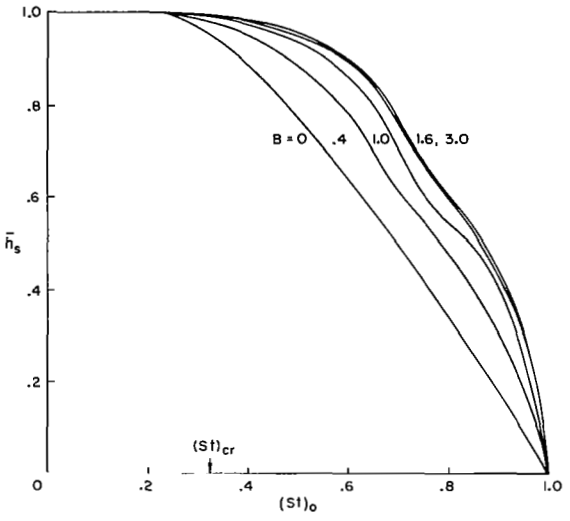

(b) The enthalpy behind the normal shock wave with air injection.

Figure 10.- The effect of postcooling on heat transfer and the flow enthalpy (air: p_s = 1 atm, T_s = 15,000° K, and $T_w \simeq 0°$ K).

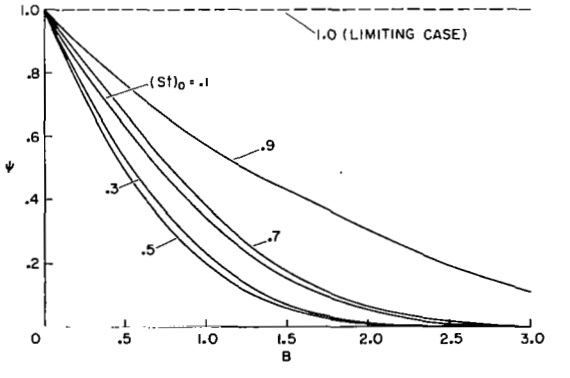

Figure 11.- The effect of Stanton number on heat reduction, air.

Stanton numbers calculated by the exact solution (eqs. (8)) and by the linearized solution of equations (10) are presented in figure 10(a) for the initial condition of p_s = 1 atm, T_s = 15,000° K, $T_w \simeq 0$, and the range of β_o^* from 10^{-1} to 10^3 ($R \simeq 10^{-2} \sim 10^2$ cm). The two calculations are very nearly identical. Note that the boundary condition behind the shock wave, h_s, for smaller values of $\beta_o^*(h_s)$ is now coupled with the postcooling effect. The result of the simple formula without the postcooling effect (eq. (15b) with $h_s \approx H$) is also presented in the same figure, and agrees well with the exact solution for $\beta_o^* \gg 1$. As can be seen from the figure, the effect of the postcooling on the convective heating becomes important for the smaller body radius (or smaller Reynolds number) and at the limit for $\beta_o^* \to 0$, Stanton number approaches unity, as for free molecule flow (or for a pointed nose).

Figure 10(b) shows the variation of the enthalpy $\bar{h}_s$ with postcooling and injection obtained from the linearized solution (eqs. (10)). The effect of the postcooling on the enthalpy becomes significant beyond the critical Stanton number, $(St)_{cr} \simeq 0.32$. For a given value of $(St)_o$ and increasing injection rates, the enthalpy is less affected by the postcooling since the conductive heat in the shock layer decreases considerably. After a sufficiently large blowing rate $B \gtrsim B_* \simeq 1.6$, the enthalpy ratio is not significantly changed.

Since the enthalpy varies with Stanton number and blowing rate, the heat reduction is altered in the manner shown in figure 11. The heat reduction, obtained from equations (10), becomes less effective as the Stanton number increases beyond the critical number, $(St)_{cr} \simeq 0.32$, and ψ

approaches the free molecule flow limit of unity. Similar results were reported in reference 8. This same effect of the Stanton number on convective heat can be expected for foreign gas injections.

CONCLUDING REMARKS

Closed-form solutions have been obtained which describe the behavior of the convective heat transfer to the stagnation point of a body with mass transfer. The shock-layer energy equation was decoupled from the momentum and continuity equations by assuming that the distribution of mass flow (normalized by the free-stream mass flow) in the shock layer was independent of the heat transfer. The energy equation was linearized by the introduction of a constant thermal and transport properties for the free-stream and injection gases (i.e., it was found that convective heating can be simply calculated by an average Peclet number obtained by integration over the temperature range in the shock layer). For the case of no radiation in the shock layer, the solutions indicate:

1. The reduction of heat transfer by mass addition can be significant. The degree of heat reduction depends upon the mass addition rate and the Stanton number for no mass addition. For a given mass addition rate the heat reduction increases with increasing Stanton number until the Stanton number reaches a value of about 0.5, at which point further increases in Stanton number decrease the heat reduction.

2. The injection of gases of low molecular weight is most effective in reducing heat transfer.

3. A mixture of injection gases is less effective in reducing heat transfer than a single gas with an equivalent molecular weight.

The present linearized theory is well substantiated by comparisons with more exact solutions and provides explicit and simple correlation equations. The linearized theory of convective heat transfer, incorporating the linearized theory of radiative heat transfer (ref. 24), now provides the basic means for solving the coupling effect between convective and radiative transfer. The present method of analysis can be used to evaluate both the net mass transfer rate (including the diffusion which will be important for lighter gases) and the shearing stress at the wall.

Ames Research Center
National Aeronautics and Space Administration
Moffett Field, Calif., 94035, Apr. 25, 1969

APPENDIX A

THE EFFECT OF BOUNDARY CONDITIONS ON HEAT TRANSFER (POSTCOOLING)

The enthalpy immediately behind a strong shock wave will be significantly altered by heat transfer at the wall when conductive heat becomes a major factor in the energy balance across the bow shock wave. Only preliminary effects of heat transfer on the viscous flow field and on the convective heat at the stagnation point will be described in this appendix.

Strong Normal Shock Relation Including Heat Conduction

For simplicity it is assumed that the strong normal shock relation applies for the case of a conducting fluid. From a conservation of energy on each side of the shock wave

$$\rho_\infty V_\infty \left(h_\infty + \frac{1}{2} V_\infty^2\right) + q_\infty = \rho_\infty V_\infty \left(h_s + \frac{1}{2} v_s^2\right) + q_s \tag{A1}$$

Since the conductive heat ahead of the shock is small ($q_\infty \simeq 0$) and $v_s \ll V_\infty$, it follows that the enthalpy behind the shock wave (including the blowing effect) becomes

$$h_s = H - q_s/\rho_\infty V_\infty \tag{A2}$$

where H represents the adiabatic enthalpy without conduction

$$H = h_\infty + \frac{1}{2} V_\infty^2 \tag{A3}$$

Dividing equation (A2) by $(H - h_w)$ and differentiating equation (8) with respect to η, one obtains the boundary enthalpy

$$\bar{h}_s = 1 - (St)e^{\int_0^1 \beta X \, d\eta_1} \qquad (h_w \simeq 0) \tag{A4}$$

Also, from equation (8), $\bar{h}_s$ becomes

$$\bar{h}_s - \bar{h}_w = (St)\left(\int_0^1 \beta e^{\int_0^{\eta_1} \beta X \, d\eta_2} \, d\eta_1\right) \tag{A5}$$

and one can obtain the Stanton number from equations (A4) and (A5),

$$(St) = \frac{1 - \bar{h}_w}{\int_0^1 \beta e^{\int_0^\eta \beta X \, d\eta_1} \, d\eta + e^{\int_0^1 \beta X \, d\eta}} \tag{A6}$$

The enthalpy behind the shock (eq. (A5)) depends upon the blowing rate as well as the Stanton number. Equation (A6) provides a closed form solution for $\beta \simeq \beta_s$, a constant. When $\beta = \beta^*(\bar{h}_s)$, equation (A6) can be solved by straightforward iteration. However, the difference in Stanton number due to changing β^* is minor since $\beta^* \simeq \beta_s^* / \sqrt{\bar{h}_s}$ for $\bar{h}_s \neq 0$.

Equation for Heat Reduction - Postcooling Effect

The reduction in convective heat with gas injection will be signifcantly affected by the postcooling phenomenon. From equation (A6) the heat reduction is calculated by

$$\psi = \frac{(St)}{(St)_o} \tag{A7}$$

It is observed from equations (A1) through (A7) that the major change in convective heat transfer due to mass addition for larger Stanton number (in effect, smaller Reynolds numbers) depends strongly upon the reduced enthalpy (driving enthalpy) accompanied by this postcooling process behind the normal shock wave.

APPENDIX B

APPROXIMATE EQUATIONS FOR THE FLOW PROPERTIES

The various physical quantities required to evaluate the linearized solutions are as follows:

Mass Flow Gradient $(\chi_w')^*$ for $T_s \gg T_w \simeq 0$

According to the potential flow and the Newtonian flow theories, the velocity gradient at the stagnation point of an axisymmetric body is approximated by (ref. 38)

$$-\left(\frac{\partial v}{\partial y}\right) = 2\left(\frac{\partial u}{\partial x}\right) \simeq \frac{2\sqrt{2(p_s - p_\infty)/\rho_s}}{R} \tag{B1}$$

For compressible flow and for $T_s \gg T_w$ it is found (ref. 23) that

$$-\left[\frac{\partial(\rho v)_w}{\partial y}\right] \simeq 2\rho_s\left(\frac{\partial u}{\partial x}\right)_\delta \tag{B2}$$

It follows that

$$(\chi_w') = 2\frac{L_o}{V_s}\left(\frac{\partial u}{\partial x}\right) \simeq k_a\gamma\sqrt{8\epsilon(1-\epsilon)} \tag{B3}$$

where

$$\left.\begin{aligned} V_s &= \epsilon V_\infty \qquad \gamma = \frac{1.187}{1 + 0.225\sqrt{\epsilon}} \\ k_a &= \frac{(L_o/R)}{\epsilon} \simeq \frac{1}{1 + \sqrt{\frac{8}{3}\epsilon} - \epsilon} \end{aligned}\right\} \tag{B4}$$

for a spherical body (see ref. 45; see also ref. 46 for nonspherical bodies); γ is a modified factor introduced in reference 47 for velocity gradient.

Mass-Flow Gradient $(\chi_w')^{**}$ for $T_s \simeq T_w$

When the wall temperature is comparable to the boundary-layer-edge temperature, the effective mass-flow gradient at the stagnation point decreases signficantly because of the higher viscous effect in the boundary layer.

Let the effective mass gradient at the wall for the case where $T_s \simeq T_w$ be $(\chi_w')^{**}$, and the thermal and transport property parameter be

$$\left(\frac{k}{c_p}\right)^{**} \equiv \frac{1}{T_s - T_w} \int_{T_w}^{T_s} \left(\frac{k}{c_p}\right) dT \tag{B5}$$

Then, the convective heat at the stagnation point for the no injection case is exactly analogous to that for $T_s \gg T_w$. It follows, by analogy with equation (14), that

$$q_{co} = \sqrt{\frac{2}{\pi} \frac{\rho_\infty V_\infty}{L_o} \left(\chi_w' \frac{k}{c_p}\right)^{**}} (h_s - h_w) \tag{B6}$$

It has been demonstrated (see refs. 26, 30, 38, and fig. 3(a)) that the heat transfer depends mainly on the enthalpy difference $(h_s - h_w)$; therefore, it can be assumed, from equations (14) and (B6), that

$$\left(\chi_w' \frac{k}{c_p}\right)^{*} \simeq \left(\chi_w' \frac{k}{c_p}\right)^{**} \tag{B7}$$

Equation (B5) can be expressed in terms of $(k/c_p)^*$, and the ratio

$$k_w = \frac{(k/c_p)^*}{(k/c_p)^{**}} = \frac{1 - \bar{T}_w}{1 - \bar{T}_w[(k/c_p)_w^*/(k/c_p)^*]} \tag{B8}$$

where

$$\bar{T}_w = \frac{T_w}{T_s}$$

From equation (B7), the effective mass-flow gradient for general wall conditions becomes

$$(\chi_w')^{**} \simeq k_w(\chi_w')^* \tag{B9}$$

This approximation is shown to be valid (fig. 4).

Shock-Layer Thickness

The shock-layer thickness L depends upon the mass injection rate. In adiabatic flow it is correlated by a simple expression (refs. 46 and 48)

$$\frac{L}{L_o} \simeq 1 + k_b \sqrt{\frac{1}{\epsilon}\left(\frac{M_\infty}{M_f}\right)}\, \chi_w \tag{B10}$$

where k_b is the shape factor that depends upon the body shape; for example, reference 48 gives $k_b \simeq 1.0$ for an axisymmetric stagnation point. Using the definition for $(St)_o$ given by equation (15a), equation (B10) can be rewritten as

$$\frac{L}{L_o} \simeq 1 + k_b \sqrt{\frac{1}{\epsilon}\left(\frac{M_\infty}{M_f}\right)}\, (St)_o B \tag{B11}$$

where the Stanton number at the stagnation point for the no injection case can be expressed simply as (e.g., see eqs. (15b) and (B22))

$$(St)_o \propto \frac{1}{\sqrt{\rho_\infty R}} \tag{B12}$$

Note that in this analysis the heat reduction equation for ψ (see, e.g., eqs. (17)) provides a correlation curve only if the Stanton number $(St)_o$ or the product $(\rho_\infty R)$ remains constant.

Boundary-Layer Thickness

An important characteristic dimension in the viscous layer is the thermal boundary-layer thickness δ. In this report the thermal thickness is arbitrarily defined as the distance from the wall where the driving enthalpy is 99 percent of its original value, that is, for $y = \delta$,

$$\frac{h_\delta - h_w}{h_s - h_w} \simeq 0.99 \qquad \frac{h_w}{h_s} \simeq 0 \tag{B13}$$

Associating equation (B13) with equation (11b), one obtains the result

$$\frac{\delta}{L} \simeq \left(\frac{\delta}{L}\right)_o + \frac{\chi_w}{(\chi_w')^*} \qquad \text{for} \quad \chi_w \ll 1 \tag{B14}$$

where the thermal layer thickness for the no injection case incorporating equation (15b) is

$$\left(\frac{\delta}{L}\right)_o = \frac{1.82}{\sqrt{\frac{1}{2}\,(\beta_o \chi_w')^*}} = \frac{1.82\sqrt{\pi}}{(\chi_w')^*}\,(St)_o \tag{B15}$$

It is interesting to compare equation (B15) with the empirical formula deduced from reference 23. The boundary-layer thickness of reference 23, with $u/u_s \simeq 0.99$, can be rewritten

$$\frac{\delta}{\sqrt{\frac{\mu_s}{2\rho_s(\partial u/\partial x)_\delta}}} \simeq 3.0 \tag{B16}$$

Equation (B15) becomes identical with equation (B16) if the Prandtl number is a constant near 0.74, which is the case treated in reference 23.

Letting the characteristic (displacement) thickness $\delta^\dagger$ be about one-half the boundary-layer thickness δ_o defined by equation (B15), one can define the critical Stanton number where the shock layer is dominated by the viscous flow and the vorticity effect so that heat conduction behind the shock wave and the terms in the flow equations of order (δ/R) are no longer negligible. Thus, this critical Stanton number $(St)_{cr}$ can be given as

$$(St)_{cr} \simeq \frac{(\chi_w')^*}{0.91\sqrt{\pi}} = 0.62\ (\chi_w')^* \tag{B17}$$

after incorporating equation (B15) with $(\delta^\dagger/L_o) \simeq 1/2\ (\delta/L_o) \simeq 1.0$.

The Blowing Parameter for the Boundary-Layer Blowoff, B_*

As the blowing rate increases, the effect of the foreign gases on heat transfer can become much stronger than that of the free-stream gas. The onset of this behavior is defined by "an effective blowoff parameter B_*," described below. The relation $\delta/L_o \simeq L/L_o - 1$ is used to replace the original boundary-layer thickness $(\delta/L)_o$ by the increase of the shock-layer thickness due to the injection. Then one obtains the result from equations (B11) and (B15) that

$$B_* \simeq 1.82\sqrt{\pi}\ \frac{\sqrt{\epsilon(M_f/M_\infty)}}{k_b(\chi_w')^*} \tag{B18}$$

For air as the free-stream gas, $(\chi_w')^* \simeq 1/2$, $\epsilon \simeq 1/16$, and it follows that

$$B_* \simeq 1.59\ \sqrt{\frac{M_f}{28.9}} \tag{B19}$$

As noted from equation (B19), the parameter B_* is independent of Stanton number, and thus of the product $\rho_\infty R$.

Equations for the Heat-Transfer Parameter

The heat-transfer rate at the stagnation point for the no injection case can, from equation (14), be written as

$$q_{co} = \frac{\sqrt{\frac{2}{\pi}\left(\chi_w'\right)^*}}{\sqrt{Pr^*Re^*}}\,\rho_\infty V_\infty (h_s - h_w) \tag{B20}$$

where

$$Pr^* = \frac{\mu^*}{(k/c_p)^*}\,, \qquad Re^* = \frac{\rho_\infty V_\infty L_o}{\mu^*}$$

and

$$\rho_\infty V_\infty = \sqrt{\frac{\frac{1}{\epsilon} + 1}{\frac{1}{\epsilon} - 1}}\,\frac{p_s - p_\infty}{\sqrt{2(H_s - h_\infty)}} \tag{B21}$$

(see ref. 24 for values of $1/\epsilon$). It can be shown that (eqs. (14), (B3), and (B21))

$$q_{co}\sqrt{\frac{R}{p_s}} = \sqrt{\frac{(4\gamma/\pi)(1 + 1/\epsilon)^{1/2}(k/c_p)^*}{(H - h_\infty)^{1/2}}}\,(h_s - h_w) \simeq \text{const.}\,(h_s - h_w) \tag{B22}$$

since $(k/c_p)^* \propto \sqrt{h_s}$ as shown in figure 2(b). Equation (B20) in dimensionless form is

$$(St)_o\sqrt{Re^*} = \sqrt{\frac{2}{\pi}\left(\chi_w'\right)^*/Pr^*} \tag{B23}$$

The present analysis on heat transfer may be expressed in term of the following simple correlation formula

$$\left.\frac{Nu}{\sqrt{Re}}\right|_x \simeq \frac{1}{\sqrt{k_a}}\left.\frac{Nu}{\sqrt{Re}}\right|_{L_o} \tag{B24}$$

where

$$\left.\frac{Nu}{\sqrt{Re}}\right|_x \equiv \frac{q_{co}x c_{pw}}{k_w(h_s - h_w)\sqrt{\rho_w u_s x/\mu_w}} \tag{B25}$$

$$\left.\frac{Nu}{\sqrt{Re}}\right|_{L_o} \equiv \frac{q_{co}L_o c_{pw}}{k_w(h_s - h_w)\sqrt{\rho_w V_s L_o/\mu_w}} \tag{B26}$$

It follows from equations (B20) and (B24) that

$$\left.\frac{Nu}{\sqrt{Re}}\right|_x \simeq \sqrt{\frac{2}{\pi}(Pr)_w}\sqrt{\frac{[(\chi_w' k/c_p)^*]/[(k/c_p)_w]}{k_a(\rho_w/\rho_s)}} \qquad (B27)$$

REFERENCES

1. Allen, H. Julian; Seiff, Alvin; and Winovich, Warren: Aerodynamic Heating of Conical Entry Vehicles at Speeds in Excess of Earth Parabolic Speed. NASA TR R-185, 1963.

2. Swann, R. T.; and Pittman, C. M.: Transient Response of Advanced Thermal Protection Systems for Atmospheric Entry. NASA TN D-1370, 1962.

3. Marvin, Joseph G.; and Pope, Ronald B.: Laminar Convective Heating and Ablation in the Mars Atmosphere. AIAA J., vol. 5, no. 2, Feb. 1967, pp. 240-248.

4. Anfimov, N. A.; and Al'tov, V. V.: Heat Transfer, Friction, and Mass Transfer in a Laminar Multicomponent Boundary Layer With Injection of a Foreign Gas. Internatl. Chemical Engineering, vol. 6, no. 1, Jan. 1966, pp. 137-144.

5. Petrov, G. I.; and Anfimov, N. A.: Flow in a Boundary Layer of a Gas Mixture. Proc. Seventh Internatl. Symp. on Space Technology and Science, Tokyo, Japan, May 15-22, 1967, AGNE Pub. Co., 1968, pp. 331-335.

6. Howe, John T.; and Sheaffer, Yvonne S.: Mass Addition in the Stagnation Region for Velocity up to 50,000 Feet Per Second. NASA TR R-207, 1964.

7. Goldberg, L.; and Scala, S. M.: Mass Transfer in the Hypersonic Low Reynolds Number Viscous Layer. R62SD07, Space Science Laboratory, General Electric Co., Jan. 1962.

8. Chen, S. Y.; Baron, J.; and Mobley, R.: Stagnation Region Gas Injection in Low Reynolds Number Hypersonic Flow. Proc. 1967 Heat Transfer and Fluid Mech. Inst., Paul A. Libby, Daniel B. Olfe, and Charles W. Van Atta, eds., Stanford Univ. Press, 1967, pp. 34-57.

9. Hidalgo, Henry: Ablation of Glassy Material Around Blunt Bodies of Revolution. ARS J., vol. 30, no. 9, Spet. 1960, pp. 806-814.

10. Adams, Mac C.: Recent Advances in Ablation. ARS J., vol. 29, no. 9, Sept. 1959, pp. 625-632.

11. Anfimov, N. A.: Laminar Boundary Layer in a Multicomponent Mixture of Gases. NASA TT F-10,038, 1966 (translation).

12. Kays, W. M.: Convective Heat and Mass Transfer. McGraw-Hill Book Co., 1966.

13. Lees, L.: Convective Heat Transfer With Mass Addition and Chemical Reactions. Presented at AGARD Combustion and Propulsion Colloquium (Palermo, Sicily), March 17-21, 1958, Pergamon Press, 1959, pp. 451-498. (Also available as GALCIT Pub. 451.)

14. Dorrance, W. H.: Viscous Hypersonic Flow. McGraw-Hill Book Co., 1962.

15. Vojvodich, N. S.; and Pope, R. B.: The Influence of Ablation on Stagnation Region Convective Heating for Dissociated and Partially Ionized Boundary-Layer Flows. Proc. 1965 Heat Transfer and Fluid Mech. Inst., Stanford Univ. Press, 1965, pp. 114-137.

16. Liu, C. S.; and Hartnett, J. P.: Influence of Dissociation on Mass Transfer Cooling in a Carbon Dioxide-Nitrogen Binary System. ASME-AICHE, Heat Transfer Conference and Exhibit, Seattle, Washington, Aug. 6-9, 1967. ASME Paper 67-HT-70.

17. Meroney, R. N.; and Giedt, W. H.: The Effect of Mass Injection on Heat Transfer From a Partially Dissociated Gas Stream. J. Heat Transfer (trans. of the ASME), vol. 89, ser. C, no. 3, Aug. 1967, pp. 205-218.

18. Libby, Paul A.; and Pierucci, Mauro: Laminar Boundary Layer With Hydrogen Injection Including Multicomponent Diffusion. AIAA J., vol. 2, no. 12, Dec. 1964, pp. 2118-2126.

19. Zeh, Dale W.; and Gill, William N.: Heat Transfer and Binary Diffusion With Thermodynamic Coupling in Variable-Property Forced Convection on a Flat Plate. AIChE J., vol. 13, no. 1, Jan. 1967, pp. 140-147.

20. Hoshizaki, H.; and Lasher, L. E.: Convective and Radiative Heat Transfer to an Ablating Body, Part I, Final Report. Rept. LMSC-4-06-66-12, LMSC, Palo Alto Res. Lab., July 1966.

21. Hanley, G. M.; and Korkan, K. D.: Approximate Inviscid, Nonadiabatic Stagnation Region Flow Field Solution. AIAA J., vol. 3, no. 8, Aug. 1965, pp. 1537-1538.

22. McCarthy, J. F.; and Hanley, G. M.: Earth Entry at Hyperbolic Velocities. AIAA Paper 68-133.

23. Matting, Fred W.: General Solution of the Laminar Compressible Boundary Layer in the Stagnation Region of Blunt Bodies in Axisymmetric Flow. NASA TN D-2234, 1964.

24. Yoshikawa, Kenneth K.: Linearized Theory of Radiative Heat Transfer for Ablating Bodies at Meteoric Speeds. Proc. Seventh Internatl. Symp. on Space Technology and Science, Tokyo, Japan, May 15-22, 1967, AGNE Pub. Co, 1968, pp. 361-405.

25. Tellep, D. M.; and Edwards, D. K.: Paper II: Radiant-Energy Transfer in Gaseous Flows. General Research in Flight Sciences, vol. I., pt. I - Fluid Mechanics, Jan. 1959-Jan. 1960. Rept. LMSD-288139, Lockheed Aircraft Corp., Missiles and Space Div., Jan. 1960.

26. Howe, John T.; and Viegas, John R.: Solutions of the Ionized Radiating Shock Layer, Including Reabsorption and Foreign Species Effects, and Stagnation Region Heat Transfer. NASA TR R-159, 1963.

27. Goldstein, M. E.: New Formulation of the Multicomponent Laminar Boundary-Layer Problem. The Physics of Fluids, vol. 10, no. 4, April 1967, pp. 823-830.

28. Hoshizaki, H.; and Wilson, K. H.: Viscous, Radiating Shock Layer About a Blunt Body. AIAA J., vol. 3, no. 9, Sept. 1965, pp. 1614-1622.

29. Chisnell, R. F.; Hoshizaki, H.; and Lasher, L. E.: Stagnation Point Flow With Radiation. LMSC 4-43-65-4, Oct. 1965.

30. Hoshizaki, H.: Heat Transfer in Planetary Atmospheres at Super Satellite Speeds. ARS Paper 2173-61. (Also available as ARS J., vol. 32, no. 10, Oct. 1962, pp. 1544-1552.)

31. Hansen, C. Frederick: Approximations for the Thermodynamic and Transport Properties of High-Temperature Air. NACA TN 4150, 1958.

32. Ibele, W. E.; Novotny, J. L.; and Eckert, E. R. G.: Prandtl Number Measurements and Thermal Conductivity, Viscosity Predictions for Air, Helium, and Air-Helium Mixtures. Univ. of Minnesota, Heat Transfer Lab., Dec. 1963.

33. Hirschfelder, Joseph O.; Curtiss, Charles F.; and Bird, R. Byron: Molecular Theory of Gases and Liquids. John Wiley and Sons, Inc., 1954.

34. Ulybin, S. A.; Bugrov, Y. P.; and Il'in, A. V.: Temperature Dependence of the Thermal Conductivity of Chemically Nonreacting Rarefied Gas Mixtures, High Temperature (trans.), vol. 4, no. 2, March-April 1966, pp. 214-217.

35. AVCO Corp., Wilmington, Mass.: Evaluation of High-Temperature Gas Transport Properties. NASA CR-575, 1966.

36. Yos, J. M.: Transport Properties of Nitrogen, Hydrogen, Oxygen, and Air to 30,000° K. RAD TM-63-7, Res. and Adv. Devel. Div., AVCO Corp., March 1963.

37. Ahtye, Warren F.; and Peng, Tzy-Cheng: Approximations for the Thermodynamic and Transport Properties of High-Temperature Nitrogen With Shock-Tube Applications. NASA TN D-1303, 1962.

38. Fay, J. A.; and Riddell, F. R.: Theory of Stagnation Point Heat Transfer in Dissociated Air. J. Aero. Sic., vol. 25, no. 2, Feb. 1958, pp. 73-85, 121.

39. Lees, Lester: Laminar Heat Transfer Over Blunt-Nosed Bodies at Hypersonic Flight Speeds. Jet Propulsion, vol. 26, no. 4, April 1956, pp. 259-269.

40. Rose, P. H.; and Stankevics, J. O.: Stagnation-Point Heat-Transfer Measurements in Partially Ionized Air. AIAA J., vol. 1, no. 12, Dec. 1963, pp. 2752-2763.

41. Pallone, A.; and Van Tassell, W.: Stagnation Point Heat Transfer for Air in the Ionization Regime. ARS J., vol. 32, no. 3, March 1962, pp. 436-437.

42. Fay, J. A.: Hypersonic Heat Transfer in the Air Laminar Boundary Layer. Paper presented at the AGARD Hypersonic Specialists' Conference, Rhode-Saint-Genèse, Belgium, April 3-6, 1962. AGARDograph 68, McMillan Press, 1964, pp. 583-605.

43. Fay, James A.; and Kemp, Nelson H.: Theory of Stagnation-Point Heat Transfer in a Partially Ionized Diatomic Gas. AIAA J., vol. 1, no. 12, Dec. 1963, pp. 2741-2751.

44. Ferri, Antonio; and Zakkay, Victor: Measurements of Stagnation Point Heat Transfer at Low Reynolds Numbers. J. Aero. Sci., vol. 29, no. 7, July 1962, pp. 847-850.

45. Hayes, Wallace D.; and Probstein, Ronald F.: Hypersonic Flow Theory. Academic Press, 1959.

46. Katzen, Elliott D.; and Kaattari, George E.: Inviscid Hypersonic Flow Around Blunt Bodies. AIAA J., vol. 3, no. 7, July 1965, pp. 1230-1237.

47. Inouye, Mamoru: Blunt Body Solutions for Spheres and Ellipsoids in Equilibrium Gas Mixtures. NASA TN D-2780, 1965.

48. Kaattari, George E.: The Effect of Simulated Ablation-Gas Injection on the Shock Layer of Blunt Bodies at Mach Numbers of 3 and 5. NASA TN D-2954, 1965.

49. Hansen, C. Frederick: Approximations for the Thermodynamic and Transport Properties of High-Temperature Air. NASA TR R-50, 1959.

TABLE I*.- $(k/c_p)/(k/c_p)_{ref}$ and $(k/c_p)^*/(k/c_p)_{ref}$

[$k/c_p = \mu/Pr$; $(k/c_p)_{ref} = 36.9 \times 10^{-6}$ lbm/sec-ft, or $= 550 \times 10^{-6}$ gm/sec-cm]

T, °K \ p, atm	100.0	10.0	1.0	0.1	0.01
1,000	0.100000E+01 .605691E+00	0.100000E+01 .605691E+00	0.100000E+01 .605691E+00	0.100000E+01 .605691E+00	0.100000E+01 .605691E+00
2,000	.145687E+01 .923954E+00	.145687E+01 .923954E+00	.145687E+01 .923954E+00	.147018E+01 .925063E+00	.155547E+01 .932170E+00
3,000	.189730E+01 .117341E+01	.206471E+01 .118814E+01	.223923E+01 .122759E+01	.220755E+01 .125944E+01	.189730E+01 .127607E+01
4,000	.256478E+01 .144087E+01	.249190E+01 .148419E+01	.218206E+01 .149119E+01	.219931E+01 .147188E+01	.270202E+01 .149702E+01
5,000	.267546E+01 .168588E+01	.248227E+01 .167247E+01	.313709E+01 .168791E+01	.332438E+01 .175475E+01	.316304E+01 .181001E+01
6,000	.278070E+01 .185401E+01	.364194E+01 .192837E+01	.365864E+01 .198598E+01	.315177E+01 .202033E+01	.256074E+01 .198097E+01
7,000	.403066E+01 .210410E+01	.397903E+01 .220394E+01	.333086E+01 .220841E+01	.288045E+01 .214764E+01	.348265E+01 .211008E+01
8,000	.431926E+01 .236908E+01	.368086E+01 .241156E+01	.319855E+01 .233058E+01	.495698E+01 .230286E+01	.815476E+01 .268611E+01
9,000	.422441E+01 .258319E+01	.354594E+01 .254053E+01	.439855E+01 .247592E+01	.910312E+01 .291219E+01	.940555E+01 .337641E+01
10,000	.404048E+01 .273753E+01	.442811E+01 .266996E+01	.885971E+01 .294323E+01	.103928E+01 .359920E+01	.942464E+01 .398819E+01
11,000	.424119E+01 .286178E+01	.895078E+01 .309010E+01	.104223E+02 .355431E+01	.106977E+02 .423596E+01	.850030E+01 .444249E+01
12,000	.491808E+01 .300033E+01	.106360E+02 .365045E+01	.113205E+02 .416510E+01	.102679E+02 .476105E+01	.764167E+01 .474184E+01
13,000	.904886E+01 .327562E+01	.118311E+02 .423563E+01	.114960E+02 .472790E+01	.941163E+01 .515283E+01	.690065E+01 .493571E+01
14,000	.118427E+02 .382166E+01	.127148E+02 .481559E+01	.111713E+02 .520327E+01	.883452E+01 .543365E+01	.605537E+01 .504802E+01
15,000	.131548E+02 .440874E+01	.131431E+02 .535472E+01	.105751E+02 .557748E+01	.836427E+01 .564653E+01	.400780E+01 .506551E+01

*Thermo-transport property of reference 49. Some changes in transport properties between references 31 and 49 have been noticed. No significant effects on the averaged quantity and heat-transfer parameter (table II) are noted.

TABLE II.- $q_{co}\sqrt{R/p_s}$, $kW/cm^{3/2}/atm^{1/2}$

T, °K \ p, atm	100.0	10.0	1.0	0.1	0.01
0	0	0	0	0	0
1,000	.124758	.124758	.124758	.124758	.124758
2,000	.260934	.260934	.260934	.266556	.274306
3,000	.424226	.441701	.499412	.587114	.719527
4,000	.658638	.793711	.927362	.990977	1.04096
5,000	1.00186	1.13792	1.22421	1.38928	1.44939
6,000	1.31813	1.49654	1.82692	2.62735	3.71610
7,000	1.70484	2.15229	3.11495	4.08941	4.38170
8,000	2.29662	3.26810	4.30187	4.65620	5.24992
9,000	3.18093	4.34950	4.87940	5.57992	6.70618
10,000	4.17155	5.01919	5.66098	6.91708	9.29398
11,000	4.97112	5.77139	6.73418	8.90170	13.0915
12,000	5.55558	6.66062	8.15515	11.7154	16.7196
13,000	6.15677	7.72790	10.0512	15.0097	18.8342
14,000	7.01739	9.03096	12.4241	17.8402	19.6352
15,000	7.96781	10.5858	15.1278	19.6961	19.8450

NASA-Langley, 1969 —— 12 A-3260

NATIONAL AERONAUTICS AND SPACE ADMINISTRATION
WASHINGTON, D.C. 20546

OFFICIAL BUSINESS

FIRST CLASS MAIL

POSTAGE AND FEES PAID
NATIONAL AERONAUTICS AN
SPACE ADMINISTRATION

"The aeronautical and space activities of the United States shall be conducted so as to contribute . . . to the expansion of human knowledge of phenomena in the atmosphere and space. The Administration shall provide for the widest practicable and appropriate dissemination of information concerning its activities and the results thereof."

— NATIONAL AERONAUTICS AND SPACE ACT OF 1958

NASA SCIENTIFIC AND TECHNICAL PUBLICATIONS

TECHNICAL REPORTS: Scientific and technical information considered important, complete, and a lasting contribution to existing knowledge.

TECHNICAL NOTES: Information less broad in scope but nevertheless of importance as a contribution to existing knowledge.

TECHNICAL MEMORANDUMS: Information receiving limited distribution because of preliminary data, security classification, or other reasons.

CONTRACTOR REPORTS: Scientific and technical information generated under a NASA contract or grant and considered an important contribution to existing knowledge.

TECHNICAL TRANSLATIONS: Information published in a foreign language considered to merit NASA distribution in English.

SPECIAL PUBLICATIONS: Information derived from or of value to NASA activities. Publications include conference proceedings, monographs, data compilations, handbooks, sourcebooks, and special bibliographies.

TECHNOLOGY UTILIZATION PUBLICATIONS: Information on technology used by NASA that may be of particular interest in commercial and other non-aerospace applications. Publications include Tech Briefs, Technology Utilization Reports and Notes, and Technology Surveys.

Details on the availability of these publications may be obtained from:

SCIENTIFIC AND TECHNICAL INFORMATION DIVISION

NATIONAL AERONAUTICS AND SPACE ADMINISTRATION

Washington, D.C. 20546